Supporting Information

A New Supramolecular Route for Using Rod-Coil Block Copolymers in Photovoltaic Applications

By *Nicolas Sary, Fanny Richard, Cyril Brochon, Nicolas Leclerc, Patrick Lévêque, Jean-Nicolas Audinot, Solenn Berson, Thomas Heiser,* Georges Hadziioannou,** and *Raffaele Mezzenga**

Copolymer synthesis

The P3HT-P4VP block copolymer has been obtained by anionic polymerization of 4-vinylpyridine and quenching with an aldehyde end-functionalized P3HT (**3**) as summarized in Scheme S1. This route has been adapted from the synthesis of a poly(phenylene vinylene) (PPV)-based block copolymer previously described[S1] and will be discussed in more details in a separate manuscript focused on the block copolymer synthesis and characterisation.

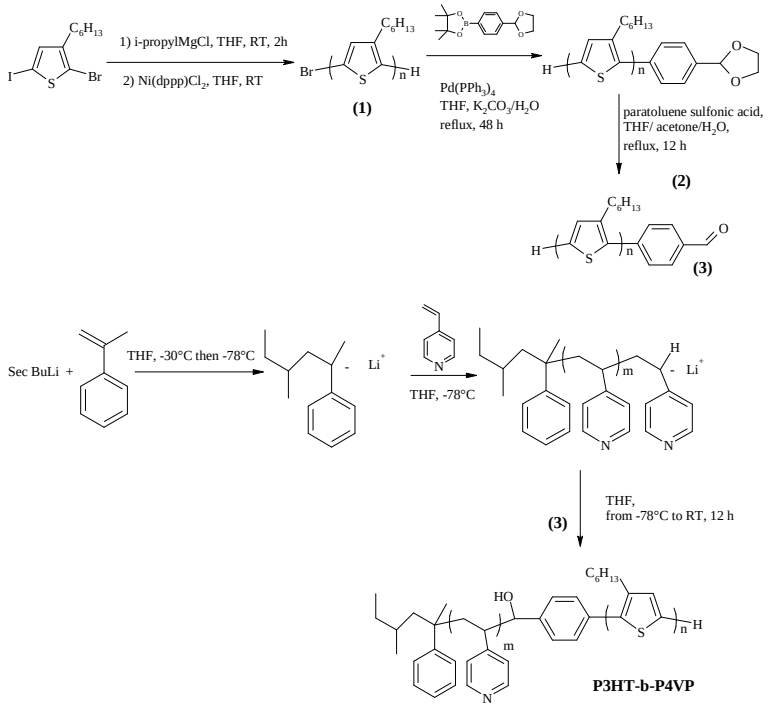

Scheme S1: Schematic representation of block copolymer synthesis

The first P3HT block (**1**) was obtained by GRIM polymerization [S2], and further functionnalized by coupling on the bromine chain end, using a well known approach[S3] in order to obtain the P3HT (**2**). Aldehyde end-functionalized P3HT (**3**) was then obtained by deprotection reaction in acid conditions. The degree of functionalization (80%) was estimated by gel permeation chromatography of a P3HT-b-PS block copolymer obtained by quenching an anionic polymerization of styrene with the aldehyde end-functionalized P3HT (**3**).

Block copolymer synthesis was done by the quenching of anionic polymerization of 4-vinylpyridine with an aldehyde end-functionalized P3HT (**3**). According to the previous published synthesis conditions [S1] a large excess of living anionic P4VP chains were used. After quenching, the P4VP homopolymer was removed by washing several times (at least 3 times) the organic phase with HCl/H_2O (pH=4). Molecular weights were not determined by GPC (due to the poor solubility of P3HT-b-P4VP copolymer), but estimated by NMR. Results are summarizes in Table S1.

Table S1: characteristics of P3HT-*b*-P4VP copolymer.

	Mn (kg/mol)*	Mn « rod » (kg/mol)*	Mn « coil (kg/mol)*
P3HT	8.7	8.7	0
P3HT-b-P4VP	11.6	8.7	2.9

* determined by 1H NMR

NMR characterizations :

- P3HT (**1**):

^{1}H RMN 400 MHz, acquisition during 16h ($CDCl_3$) : δ (ppm) 0.91 (t, n*3H, aliph. CH_3); 1.33 (m, n*6H, aliph. CH_2); 1.69 (m, n*2H, aliph. CH_2); 2.6 et 2.8 (m, n*2H, aliph. CH_2); 6.98 (s, n*1H arom. CH); (n : degree of polymerization).

^{13}C RMN ($CDCl_3$): δ (ppm) 139.9; 133.7; 130.5; 128.6; 31.7; 30.5; 29.5; 29.25; 22.6; 14.1.

- P3HT (**2**) :

^{1}H RMN 400 MHz, acquisition during 16h ($CDCl_3$) : δ (ppm) 0.91 (t, n*3H, aliph. CH_3); 1.33 (m, n*6H, aliph. CH_2); 1.69 (m, n*2H, aliph. CH_2); 2.6 et 2.8 (m, n*2H, aliph. CH_2); 4.1 (m, 4H, OCH_2 chain end); 5.87 (s, 1H CH chain end); 6.98 (s, n*1H arom. CH); 7.50 (d, 2H arom. CH of chain end); 7.53 (d, 2H arom. CH of chain end); (with n being the degree of polymerization).

- P3HT (**3**) :

^{1}H RMN 400 MHz, acquisition during 16h ($CDCl_3$) : δ (ppm) 0.91 (t, n*3H, aliph. CH_3); 1,33 (m, n*6H, aliph. CH_2); 1.69 (m, n*2H, aliph. CH_2); 2.6 et 2.8 (m, n*2H, aliph. CH_2); 6.98 (s, n*1H arom. CH); 7.64 (d, 2H arom. CH chain end); 7.93 (d, 2H arom. CH chain end); 10.05 (s, 1H aldehyde OCH).

- P3HT-b-P4VP block copolymer:

^{1}H RMN 400 MHz, acquisition during 16h ($CDCl_3$) : δ (ppm) 0.91 (t, n*3H, aliph. CH_3, P3HT); 1.33 (m, n*6H, aliph. CH_2, P3HT); 1.69 (m, n*2H, aliph. CH_2, P3HT); 2.6 and 2.8 (m, n*2H, aliph. CH_2, P3HT); 6.28-6.4 (m, x*2H arom. CH, 4-VP); 6.98 (s, n*1H arom. CH, P3HT); 8.25-8.4 (m, m*2H arom. CH, 4-VP); (with n being the degree of polymerization of P3HT block and m the degree de polymerization of P4VP).

Dynamic Secondary Ion Mass Spectrometry (D-SIMS)

The active layers used for photovoltaic purposes were characterized by Dynamic Secondary Ion Mass Spectrometry (D-SIMS) with low energy impact. The experiments reported here were carried out in ultra-high vaccum (UHV) using a Cs^+ primary ion source at impact energy of 500 eV with negative ion detection to optimize the secondary detection. The ^{12}C SIMS signal was used to identify the polymer layer while the $^{12}C^{14}N$ SIMS signal was chosen to probe P4VP.

The $^{12}C^{14}N$ signal is normalized by the matrix signal (^{12}C) to follow the evolution of the concentration of nitrogen in the different layers.

SIMS depth profiles obtained on a P3HT-P4VP:PCBM/PEDOT:PSS layers, deposited on an oxidized silicon wafer, probing ^{28}Si (crosses), ^{12}C (open squares), ^{16}O (close triangles) and $^{12}C^{14}N$ (close circles) are shown in Figure S1 and S3 for C8 and C17, respectively. *Insert* : $^{12}C^{14}N$ signal normalized by the ^{12}C signal (polymer matrix), to attenuate a possible matrix effect.

Both interfaces with the PEDOT:PSS layer can be clearly identified : the PEDOT:PSS /SiO_2 interface is marked by the rapidly increasing ^{28}Si signal, while the P3HT-P4VP:PCBM/PEDOT:PSS interface is shown by the drop in the ^{12}C signal. Importantly, the significant increase of the $^{12}C^{14}N/^{12}C$ signal ratio close to the PEDOT:PSS layer can be attributed to P4VP accumulation at the interface. A similar peak in the distribution of ^{16}O can also be observed and could be explained by a local increase in PCBM concentration.

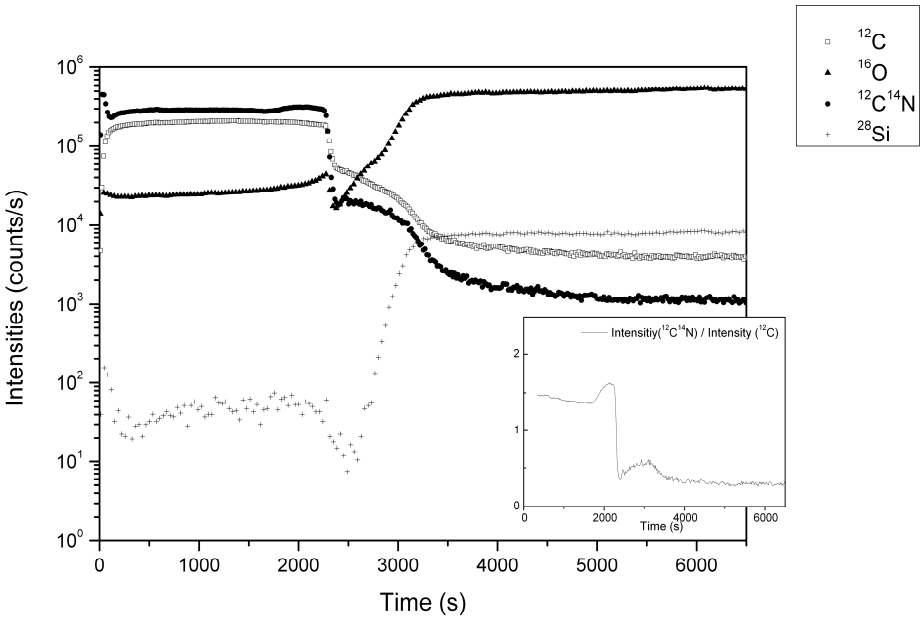

Figure S1: SIMS depth profiles obtained on a P3HT-P4VP:PCBM/PEDOT:PSS active layer with 8 % of PCBM (equivalent to C8), deposited on an oxidized silicon wafer, probing ^{28}Si (crosses), ^{12}C (squares), ^{16}O (triangles) and $^{12}C^{14}N$ (circles). *Insert* : $^{12}C^{14}N$ signal normalized by the ^{12}C signal (polymer matrix), to attenuate a possible matrix effect.

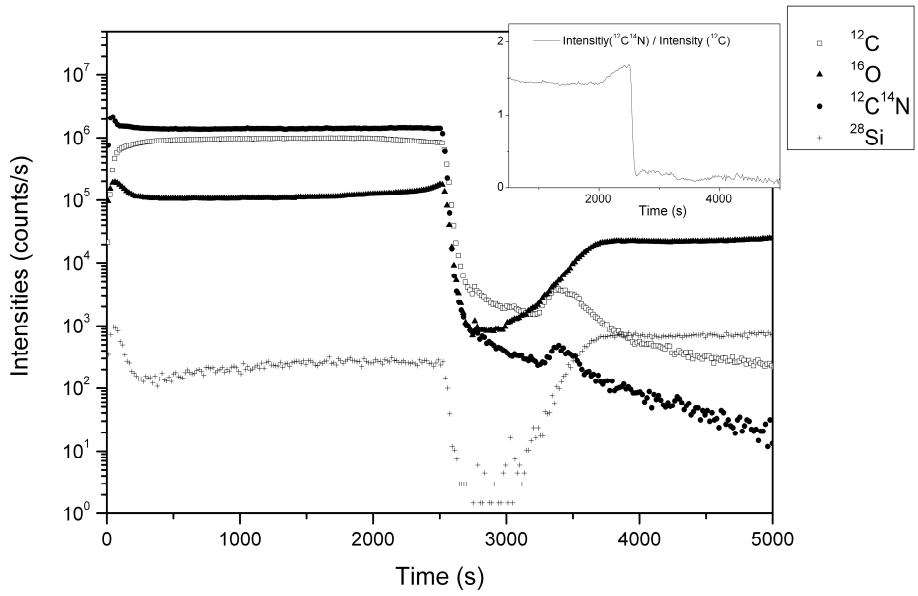

Figure S2: SIMS depth profiles obtained on a P3HT-P4VP:PCBM/PEDOT:PSS active layer with 17 % of PCBM (equivalent to C17), deposited on an oxidized silicon wafer, probing ^{28}Si (crosses), ^{12}C (squares), ^{16}O (triangles) and $^{12}C^{14}N$ (circles). *Insert* : $^{12}C^{14}N$ signal normalized by the ^{12}C signal (polymer matrix), to attenuate a possible matrix effect.

Standard device performances

Table S2 reports blend compositions and major photovoltaic parameters for devices using various P3HT-P4VP/PCBM blends.

Table S2

	C8	C17	C36
%vol PCBM (overall)	8	17	36
%vol PCBM (vs 4VP)	31	78	216
%vol PCBM (vs P3HT)	11	28	76
J_{SC} (mA/cm^2)	0.21	0.43	0.71
V_{OC} (V)	0.33	0.29	0.29
FF	30%	21%	14%
Energy Conversion Efficiency	0.017%	0.026%	0.026%

Incident-photon to current conversion efficiencies

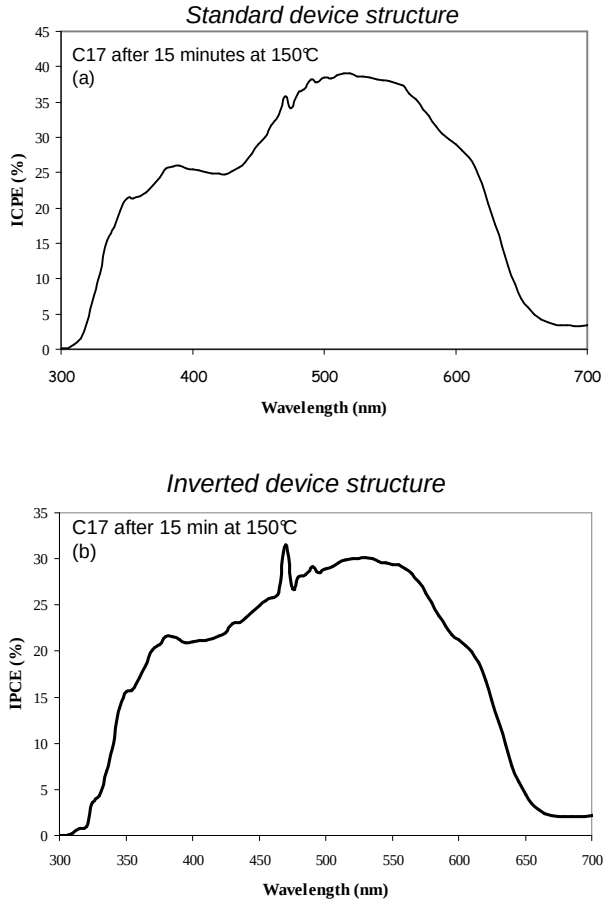

Figure S3. Incident photon-to-current conversion efficiency (or IPCE) for the C17 active layer in a standard device structure (a) and inverted device structure (b). The peak at 480 nm is an artefact due to the mono-chromator (grating exchange)

References

[S1] N. Sary, L. Rubatat, C. Brochon, G. Hadziioannou, J. Ruokolainen, R. Mezzenga, *Macromolecules* **2007**, *40*, 6990.

[S2] R. Miyakoshi, A. Yokoyama, T. Yokozawa, *J. Am. Chem. Soc.* **2005**, *127*, 17542

[S3] J. Liu, R.D. McCullough *Macromolecules* **2002**, *35*, 9882.